In Vivo Stability and Photodynamic Efficacy of Fluorinated Bacteriopurpurinimides Derived from Bacteriochlorophyll-a

Amy L. Gryshuk,[†,‡] Yihui Chen,[†] William Potter,[†] Tymish Ohulchansky,[§] Allan Oseroff,*[,‡] and Ravindra K. Pandey*[,†,||]

Photodynamic Therapy Center, Department of Dermatology, and Department of Nuclear Medicine/Radiology, Roswell Park Cancer Institute, Buffalo, New York 14263, and Institute for Lasers, Photonics and Biophotonics, SUNY at Buffalo, Buffalo, New York 14260

Received September 16, 2005

The stable bacteriopurpurinimide (788 nm, ϵ: 38 600 in CH_2Cl_2), obtained by reducing the corresponding unstable Schiff base (803 nm, ϵ: 50 900 in CH_2Cl_2) that was isolated by reacting bacteriopurpurin methyl ester with 3,5-bis-(trifluoromethyl)benzylamine, produced promising photosensitizing efficacy. ^{1}H NMR, mass spectrometry, and HPLC analyses confirmed the structures of new bacteriopurpurinimides and the metabolic product. The preliminary in vivo photosensitizing efficacy of this stable bacteriopurpurinimide was determined in C3H mice bearing radiation induced fibrosarcoma tumors as a function of variable drug doses. A drug dose of 1.0 μmol/kg and light exposure of 135 J/cm^2 (75 mW/cm^2; 24 h postinjection) at 796 nm for 30 min produced a 60% long-term tumor cure (3/5 mice were tumor-free on day 90). Colocalization study of the stable bacteriopurpurinimide with MitoTracker Green confirmed some mitochondrial localization. The fluorescein-exclusion assay and histological staining of CD31 confirmed vascular stasis at various time points post-PDT (post photodynamic therapy). The treatment parameters (time for maximum drug uptake and wavelength for light irradiation) were determined by in vivo reflectance spectroscopy.

Introduction

Photodynamic therapy[1−4] (PDT) involves the administration of photosensitizer (PS) either systemically or locally, followed by illumination with light. The PS absorbs the light and, in the presence of oxygen, produces cytotoxic oxygen species, which are believed to be a key element that destroys the tumor cells.[5,6] The penetration of light through tumor tissue is highly complex due to the interactions of the light with the absorbing and highly scattering medium.[7] As light enters tissue at more than 2 or 3 mm the photon becomes diffuse (i.e. nondirectional), such that light penetration is governed by either intrinsic scattering or absorption per unit path. Absorption is necessary in PDT where the photon is absorbed so that the photochemical reaction is generated. For instance, each layer of the tumor tissue medium absorbs "an equal fraction of the light passing through it, but the amount of light it receives is successively decreasing".[8] However, the penetration of light in tumor tissue increases as the wavelength of light increases from 600 to 800 nm.[8] The probability per unit path length of a photon being absorbed by an endogenous chromophore, such as water, hemoglobin, deoxyhemoglobin, and melanin (wavelengths shorter than 630 nm), decreases with increasing wavelength (700 to 800 nm). The strong peaks of the absorption bands of hemoglobin and deoxyhemoglobin are found at wavelengths shorter than 630 nm. The tails of these bands extend beyond 630 nm and become weaker with increasing wavelength. The other endogenous chromophore, melanin, absorbs light over a broad range of wavelengths throughout the visible and near-infrared, but is fortunately not present in significant amounts in most tissues.[7,8] Therefore, during therapeutic applications, for maximum penetration it is best to use red light excitation near 800 nm.

From the studies of various porphyrin and phthalocyanine-based compounds,[9,10] it is now well accepted that the overall lipophilicity of the molecule and position of substituents play important roles in their in vivo photosensitizing activity.[11−14] For the past several years, one of the objectives of various investigators has been to develop photosensitizers with long-wavelength absorption near 800 nm.[9,10,15] In our previous studies, we have shown that unstable bacteriochlorophyll-a, present in *Rhodobacter sphaeroides*, can be converted into a stable bacteriopurpurinimide where some of the related alkyl ether derivatives were found to be quite effective, both in vitro and in vivo.[16] In our attempt to establish a structure/activity relationship (SAR) in the purpurinimide series, we observed that, among certain *N*-aryl substituted analogues, the fluorinated purpurinimides showed enhanced in vivo efficacy, compared to the corresponding nonfluorinated derivatives.[17] Due to a close structural relationship between the purpurinimide (one pyrrole ring is reduced) and the bacteriopurpurinimide systems (two pyrrole rings diagonal to each other are reduced), we extended this approach to bacteriopurpurinimides, with an aim to establish a generic structural requirement for effective photosensitizers. In this manuscript the synthesis, stability, tumor uptake, intracellular localization, and in vitro/in vivo photosensitizing efficacy of the fluorinated bacteriopurpurinimides obtained by reacting bacteriopurpurin-18 with a large excess of 3,5-bis-(trifluoromethyl)benzylamine and the corresponding reduced product are described.

Results and Discussion

Chemistry. Bacteriopurpurin methyl ester **1** was isolated from *Rb. sphaeroides* by following the methodology developed in our laboratory.[18] Reaction of **1** (Scheme 1) with 3,5-bis-(trifluoromethyl)-benzylamine in refluxing benzene (dried over sodium) under nitrogen atmosphere produced a mixture of two compounds, which were separated by preparative thin-layer chromatography using 3% methanol/CH_2Cl_2 as a mobile phase. The faster moving band was identified as bacteriopurpurin-18-*N*-3,5-bis(trifluoromethyl)benzylimide methyl ester (λ_{max} 824

* Authors to whom correspondence should be addressed. R.K.P.: phone, 716-845-3203; fax, 716-845-8920; e-mail, ravindra.pandey@roswellpark.org. A.O.: phone, 716-845-5813; fax, 716-845-5780; e-mail, allan.oseroff@roswellpark.org.

† Photodynamic Therapy Center, Roswell Park Cancer Institute.

‡ Department of Dermatology, Roswell Park Cancer Institute.

§ SUNY at Buffalo.

|| Department of Nuclear Medicine/Radiology, Roswell Park Cancer Institute.

10.1021/jm050919z CCC: $33.50
Published on Web 02/18/2006

Scheme 1

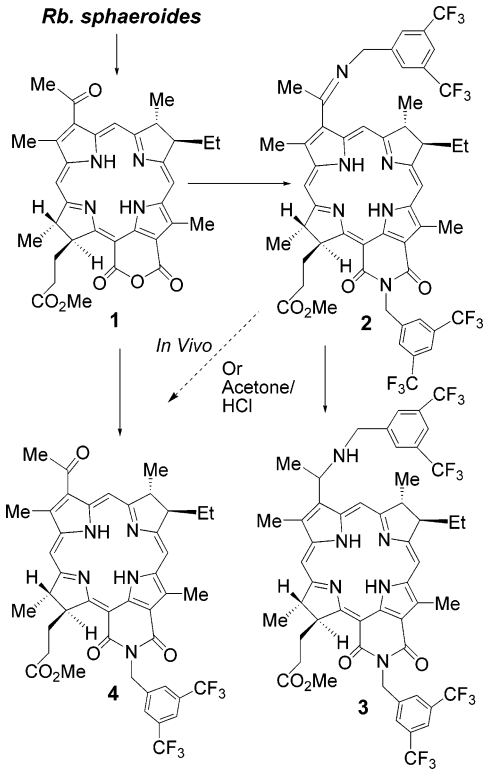

nm, ϵ: 71 444 in CH_2Cl_2) **4**, and the slower moving compound was characterized as 3^1-3,5-bis(trifluoromethyl)benzylimine-bacteriopurpurin-18-*N*-3,5-bis(trifluoromethyl) benzyl imide **2** (λ_{max} 803 nm, ϵ: 50 900 in CH_2Cl_2). The ratios for the formation of these products were found to be dependent on the reaction conditions and the amount of the reactants used. The reduction of the Schiff base **2** with sodium borohydride produced the corresponding amine **3** (λ_{max} 788 nm, ϵ: 38 600 in CH_2Cl_2), with a significant hypsochromic shift in the electronic absorption spectrum (Figure 1).

In another set of experiments, treatment of the Schiff base **2** in acetone/aqueous HCl produced the corresponding acetyl analogue **4**, which further confirmed its proposed structure. The ^{1}H NMR and the mass spectrometry analyses confirmed the structures of new bacteriopurpurinimides **2**−**4**. Analytical TLC and HPLC analyses ascertained the purity of the reaction products.

Determination of in Vivo Stability of Bacteriopurpurinimide 2. The stability, the comparative drug uptake in tumor vs skin, and the changes in the in vivo electronic absorption spectra of new bacteriopurpurinimides were determined by in vivo reflectance spectroscopy, which offers the same advantages as a double-beam absorption spectrophotometer.[19]

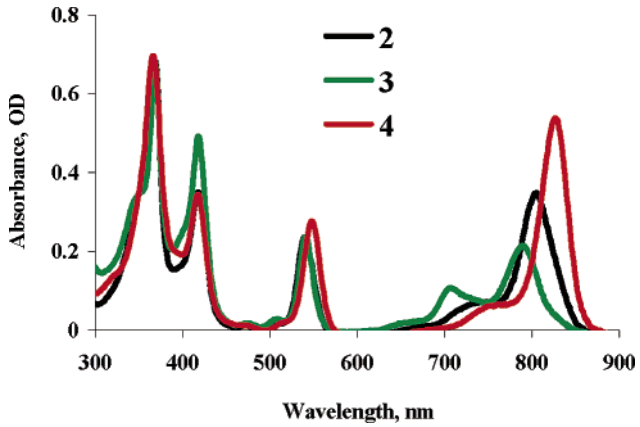

Figure 1. Electronic absorption spectra of bacteriopurpurinimides **2**−**4** in dichloromethane.

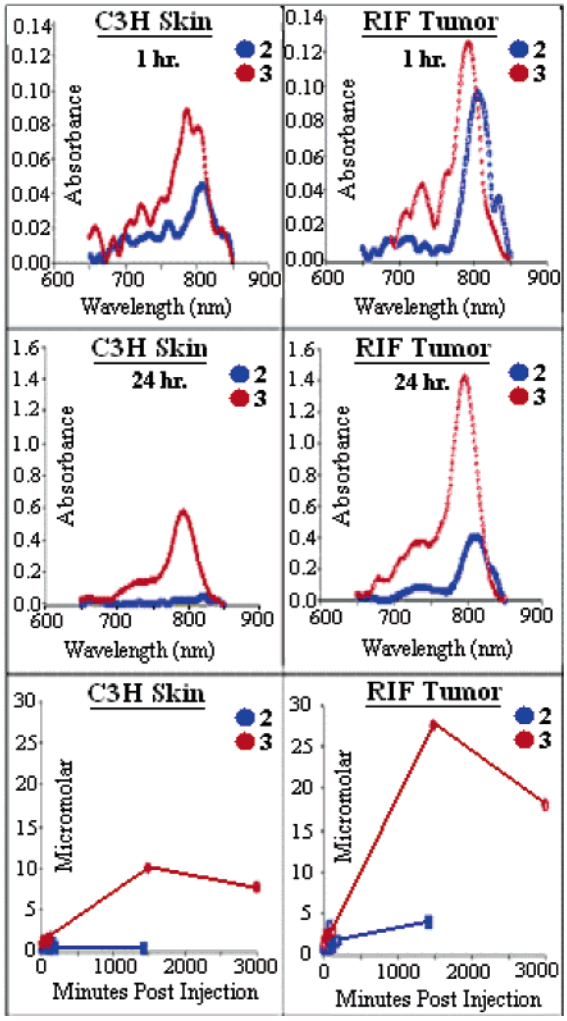

Figure 2. Stability and tumor vs skin uptake of photosensitizers **2** and **3** determined by in vivo reflectance spectroscopy in C3H mice bearing RIF tumors.

The preinjection mouse data can be thought of as the reference beam sample and the postinjection data as the sample beam containing everything in the reference beam plus the experimental drug. It has been previously shown that the absorption spectrum of a compound in a living tissue is extremely valuable in determining its in vivo stability and concentration in tumor and adjacent skin. For a photosensitizer to be considered biologically active under PDT conditions, it is necessary that it display stability and significantly enhanced tumor selectivity. Bacteriopurpurinimide **2** exhibited some interesting properties. Upon initial injection, **2** already exhibited two peaks characteristic of in vivo cleavage of the C═N bond by water (Figure 2). Over time, **2** slowly displayed evidence of conversion to its metabolite **4**, which exhibited a shoulder peak shift from ~803 to ~826 nm. On the other hand, the corresponding reduced bacteriopurpurinimide **3** was quite stable, which was further confirmed by HPLC analyses (Figure 3).

A red shift in the long-wavelength absorption band for compound **3**, from 788 nm in vitro to 796 nm in vivo, apparently reflects its binding to various tissue components. From the results obtained by the in vivo reflectance spectroscopy it was evident that bacteriopurpurinimde **3** was at a greater level in

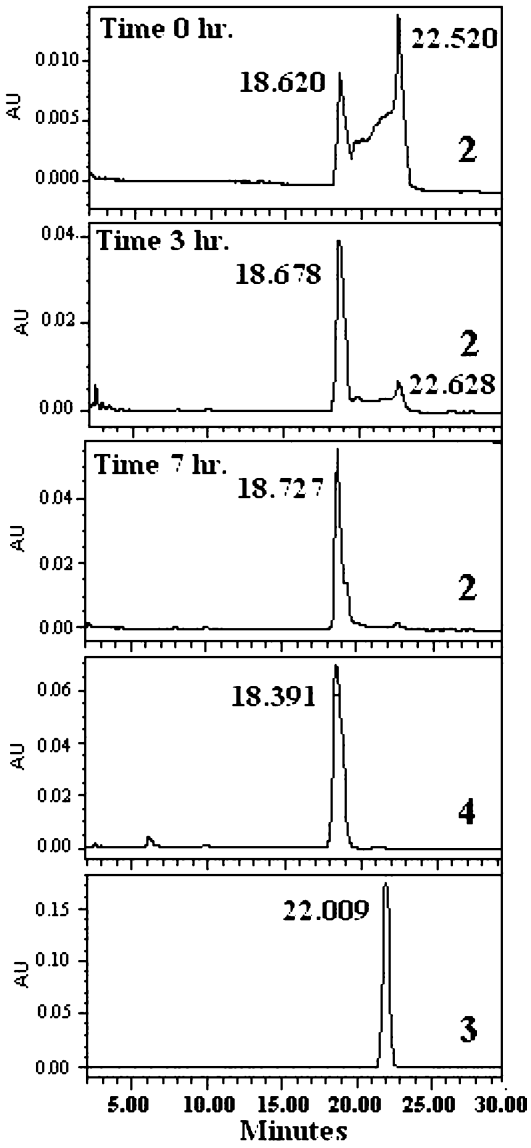

Figure 3. HPLC analyses of photosensitizers **2**−**4**.

the tumor at 24 h (∼1440 min) compared to that at 48 h (∼3000 min). Drug accumulation was also more selective for the radiation induced fibrosarcoma (RIF) tumor compared to the C3H skin (3:1 respectively) at 24 h postinjection.

Determination of Drug Stability by HPLC Analysis. The results obtained from HPLC analysis suggest that bacteriopurpurinimide **2** is unstable in its 1% Tween 80/D5W formulation. Leaving the solution at room temperature for a few hours converted it into bacteriopurpurinimide **4**, which was also identified as an in vivo metabolic product by reflectance spectroscopy.

As can be seen from Figure 3, by HPLC analysis, bacteriopurpurinimide **4** displayed a single peak at 18.39 min, whereas **2** displayed two distinct peaks with retention time of 18.62 and 22.52 min. On leaving **2** in its 1% Tween 80/D5W formulation at room temperature over time (30 min to 29 h), a significant difference in peak intensity at two different time points was observed. For example, at 3 h, **2** displayed a significant increase in the 18.62 min peak, with a continued decrease in the peak at 22.52 min. After leaving the solution for 7 h, there was a near disappearance of the 22.52 min peak, confirming that the Schiff base **2** was unstable when either left at room temperature or stored at 4 °C for a long period of time in solution and

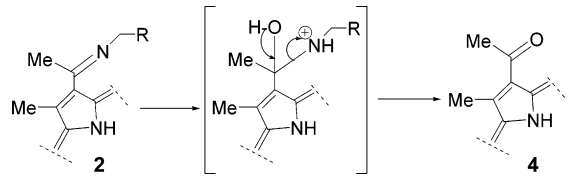

Figure 4. A possible mechanism for the in vivo conversion of compound **2** to **4.**

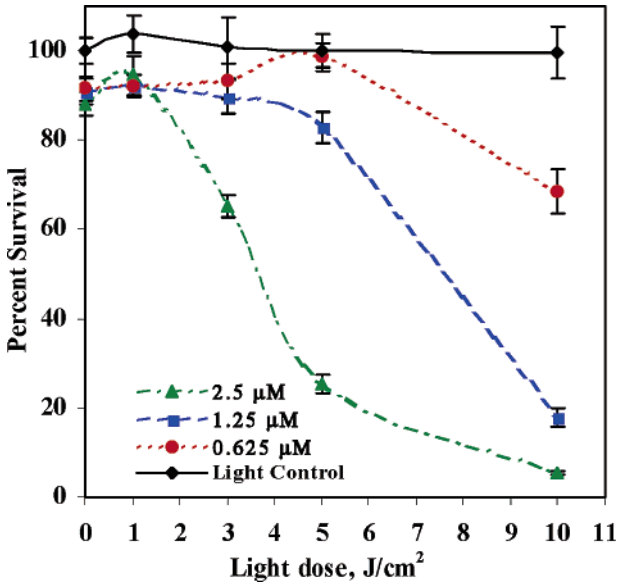

Figure 5. MTT assay (48 h postillumination) of **3** in RIF cells with varying drug concentrations (0.6−2.5 μM) and the light dose of 0−10 J/cm^2 at a dose rate of 3.2 mW/cm^2.

completely converted into the corresponding 3-acetyl derivative **4**. On the other hand, the corresponding reduced bacteriopurpurinimide **3** was found to be quite stable in solution and a single HPLC peak was observed at 22.009 min.

The mechanism of the formation of the metabolite could be due to the nucleophilic attack of water at the 3^1-position and subsequent cleavage of the carbon−nitrogen bond leading to its conversion into the corresponding acetyl analogue **4** (Figure 4).

In Vitro Photosensitizing Efficacy. As can be seen from Figure 5, the bacteriopurpurinimide **3** produced a dose- and light-dependent PDT response as determined by the MTT assay.[20] Bacteriopurpurinimide **4** could not be evaluated at this time due to laser limitations (not enough power to treat at ∼824 nm). Therefore only bacteriopurpurinimide **3** was taken into further in vivo investigation.

Intracellular Localization. The literature survey revealed that, among tetrapyrrole-based compounds, the most effective photosensitizers tend to localize either in mitochondria or in lysosomes.[21] And in general, compounds that localize in mitochondria were found to be more effective.[22] Therefore, to investigate the site of localization of new bacteriopurpurinimide **3**, the RIF cells were coincubated with the photosensitizer and MitoTracker Green (a mitochondria localizing probe). As can be seen from Figure 6, after a 24 h incubation, **3** was found to be partially localized in the mitochondria. Other site(s) of localization were not determined at this time.

In Vivo Photosensitizing Efficacy. In order to determine the optimal drug dose, bacteriopurpurinimide **3** was evaluated at three drug doses (1.0, 0.4, and 0.2 μmol/kg), and the results are summarized in Figure 7.

At 24 h postinjection, the mice (5 mice/group) were treated with laser light at 796 nm under the specified in vivo conditions

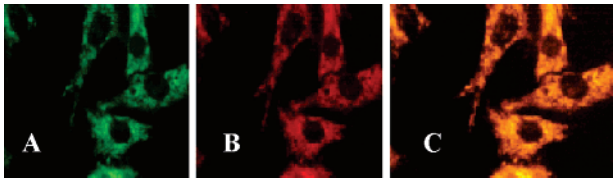

Figure 6. Intracellular localization of bacteriopurpurinimide **3** (1.0 μM) at 24 h incubation in RIF cells: (A) MitoTracker Green (100 nM); (B) compound **3**; (C) overlay of A and B.

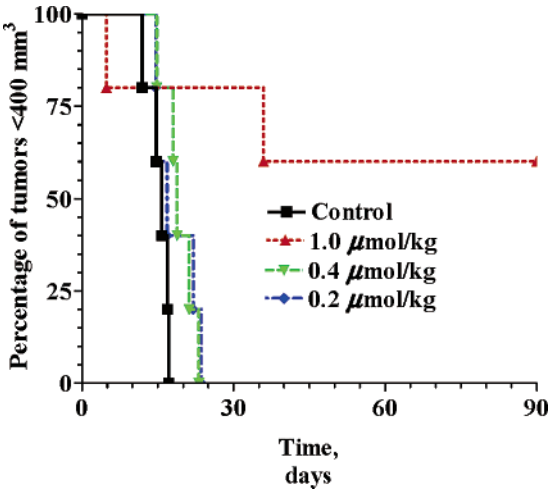

Figure 7. In vivo photosensitizing efficacy of **3** in RIF/C3H mice at varying drug doses at 24 h postinjection. PDT parameters: wavelength 796 nm, 135 J/cm^2 and 75 mW/cm^2 for 30 min.

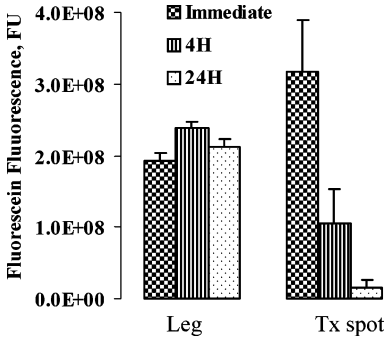

Figure 8. PDT induced vascular stasis in normal C3H mouse skin.

for a total light dose of 135 J/cm^2 at a fluence rate of 75 mW/cm^2. As can be seen, at a dose of 1.0 μmol/kg, a 60% tumor response was observed on day 90 (i.e. three out of five mice were tumor-free with no palpable tumor on day 90). Under similar treatment conditions, **3** at a dose of 0.4 and 0.2 μmol/kg did not produce any significant PDT effect.

Fluorescein-Exclusion Assay for Vascular Stasis. The fluorescein-exclusion assay was used to quantitatively determine PDT-induced vascular damage in normal mouse skin tissue.[23,24] As can be seen in Figure 8, immediately post-PDT, there was no exclusion of the fluorescein dye in the treatment site, noting that the blood vessels were initially compromised and leaky after PDT. At 4 h post-PDT, only partial fluorescein dye exclusion was observed in the treatment site compared to the hind leg (no light). In contrast, at 24 h post-PDT, there was almost complete exclusion of fluorescein fluorescence in the treatment site compared to the hind leg, noting that the vasculature had been damaged and almost completely shut down.

Confirmation of Vascular Stasis with CD31 Staining. To confirm the results that were observed by fluorescein-exclusion

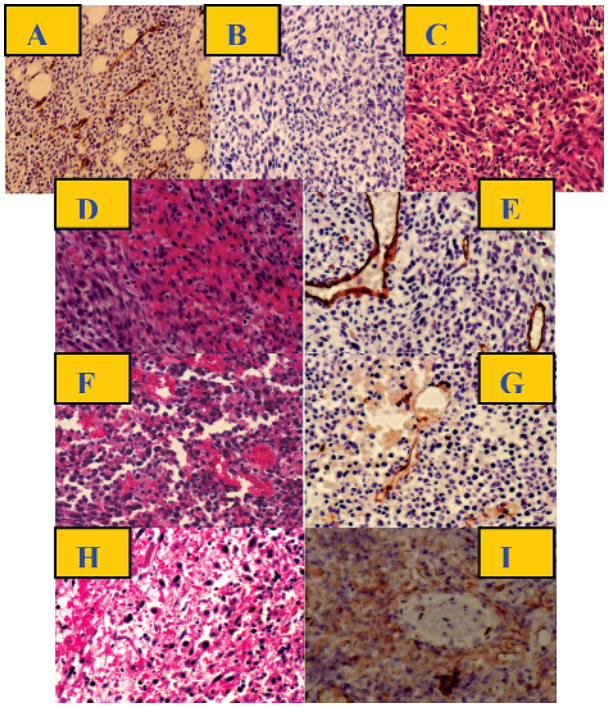

Figure 9. In vivo histochemical staining (H&E and CD31) of **3** at post-PDT. Slides: (A) +CD31 control tumor; (B) −IgG control tumor; (C) H&E control tumor; (D) H&E immediately post-PDT; (E) CD31 immediately post-PDT; (F) H&E 4 h post-PDT; (G) CD31 4 h post-PDT; (H) H&E 24 h post-PDT; (I) CD31 24 h post-PDT.

assay, tumor sample slices were stained with H&E, as well as CD31, and analyzed for tumor response post-PDT (Figure 9).[25]

The control tumors (24 h drug incubation; no light) stained positively for CD31, noting functional blood vessels in the absence of light. The H&E staining indicated that the drug alone had no significant effect on morphology of the tumor cells. Prior to PDT, the tumor was well perfused and maintained viable cells. Immediately post-PDT, the vasculature was greatly reduced. There was evidence of dilated vessels, and the H&E displayed severe edema. At 4 and 24 h post-PDT, the evidence of vascular damage was more evident. At 24 h, no functional blood vessel was found by CD31 staining, except for remnants of dilated and congested nonfunctional blood vessels. By H&E there seemed to be a large number of cells that were pycnotic, while there were a few remaining viable cells. Even though there was significant cell loss, the apparent viable cells remained to give rise to those cells that allowed for tumor regrowth. At day 90, only 60% of the mice were tumor-free (1.0 μmol/kg).

Skin Photosensitivity. One of the major problems associated with porphyrin-based compounds is long-lasting skin photosensitivity. The foot pad of SWISS/Cr mice was utilized for determining drug + light photosensitivity (Figure 10).[26] Bacteriopurpurinimde **3** was evaluated at its therapeutic dose of 1.0 μmol/kg. After a 24, 48, 72, and 96 h drug incubation, the foot was exposed to solar simulated light for 30 min (3 mice/time point) and monitored postillumination for skin photosensitivity. There was evidence of skin photosensitivity (0.35 with slight edema) at day 1 following light illumination in those mice that had been exposed to the photosensitizer for a 24 h incubation period. In those mice that had been administered the photosensitizer for 48, 72, and 96 h, there seemed to be no apparent difference from a normal mouse foot by day 1 following light illumination. These findings demonstrated that bacteriopurpurinimide **3** was specific for the tumor (by 24 h

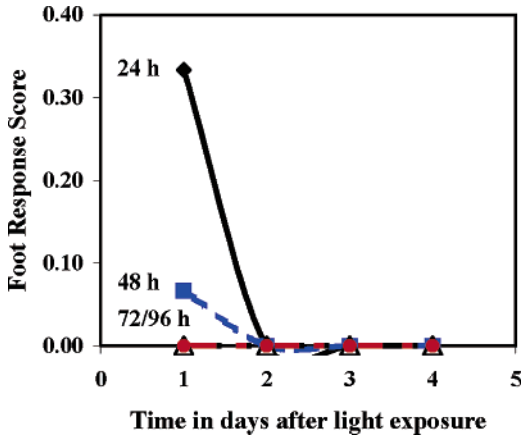

Figure 10. Skin photosensitivity of **3** in Swiss mice (1.0 μmol/kg) at variable time points postinjection (3 mice/group). The foot response was judged using a 0−3 scale (see the text).

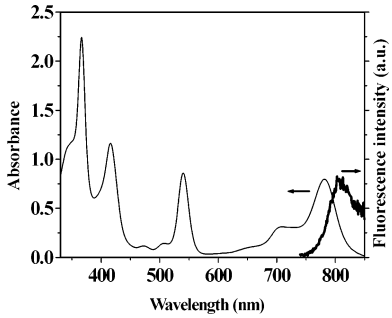

Figure 11. Absorption and fluorescence spectra of **3** in MeOH.

uptake), yet cleared at an acceptable time in which there was no evidence of severe damage to normal tissue.

Photophysical Characterization. Rhodamine 6G and Rose Bengal were used as references for the fluorescence and singlet oxygen yield measurements. During these measurements optical densities of the sample solutions in methanol were matched at the wavelength of excitation (532 nm). The fluorescence quantum yield (Φ_{Fl}) for Rhodamine 6G in methanol is 0.93,[27] and the singlet oxygen yield (Φ_{Δ}) for Rose Bengal in methanol is 0.80.[28]

The absorption spectrum of **3** in MeOH was similar to that obtained in CH_2Cl_2 solution. The position of the long-wavelength absorption peak was slightly blue-shifted in comparison to CH_2Cl_2 solution (~782 nm). The sample solution also displayed a fluorescence band with maximum at ~808 nm, which satisfied the mirror image rule with absorption band (Figure 11). The quantum yield of fluorescence was quite low (~0.03).

The singlet oxygen phosphorescence spectrum of **3** with Rose Bengal as a reference is depicted in Figure 12. Considering that the value for singlet oxygen yield for Rose Bengal in MeOH is 0.80, the singlet oxygen yield for bacteriopurpurinimide **3** in MeOH was determined as ~0.28.

The above experiments emphasized that long-wavelength photosensitizers with effective in vitro and in vivo activity can be synthesized efficiently from bacteriochlorophyll-a. These new bacteriopurpurinimides displayed improved spectroscopic properties exhibiting long-wavelength absorption near the infrared region of the electromagnetic spectrum, which should exhibit reduced absorption and scattering in tissue and provide light penetration deeper into the tissue than compounds such as Photofrin, which absorbs at ~630 nm.

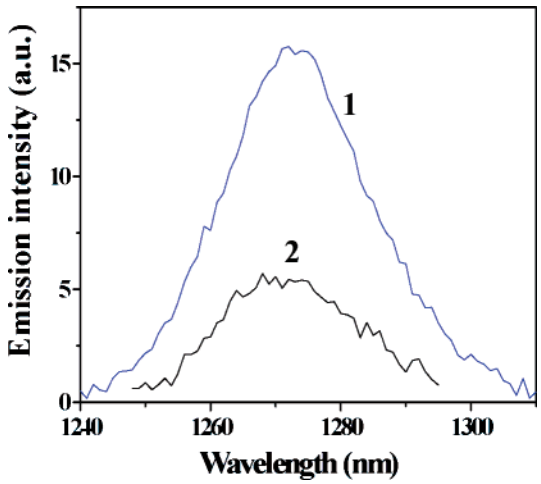

Figure 12. Spectra of singlet oxygen phosphorescence sensitized by Rose Bengal (1) and **3** (2). Spectra were corrected with background subtraction.

The Schiff base **2**, formed by reacting the bacteriopurpurinimide with a melt of 3,5-bis-(trifluoromethyl)benzylamine, was found to be unstable in vivo. Its unstable nature and the identification of the in vivo metabolite were further confirmed by IRS and HPLC analyses. However, the corresponding reduced form **3** was found to be quite stable, and this product was further investigated for its in vitro and in vivo activity. The best time for the light treatment (24 h) and the in vivo absorption of the longest wavelength (796 nm) were identified by in vivo reflectance spectroscopy.

Both in vitro and in vivo experiments displayed a dose-dependent response. In vivo, the most effective tumor response was evident as the dose escalated from 0.2 to 1.0 μmol/kg (135 J/cm^2 at 75 mW/cm^2), in which 60% of the C3H mice were tumor-free by day 90. The RIF lack the ability to undergo apoptosis. Therefore, the PDT-induced effect on vasculature was confirmed via the fluorescein-exclusion assay and CD31 staining. Interestingly, our results from both experiments displayed that, immediately following PDT, there was vessel dilation and by 24 h there was almost complete vessel ablation. On the basis of these findings, at a dose of 1.0 μmol/kg and 135 J/cm^2 at 75 mW/cm^2, our treatment was confined to photodynamic damage to the vasculature feeding the tumor. Our study indicates that vascular destruction, through blood stasis and hemorrhaging, possibly starved the tumor cells of oxygen and nutrients necessary to facilitate the tumor's survival.

In summary, we have developed an efficient approach for the preparation of a highly stable bacteriopurpurinimide with required photophysical and phototherapeutic potential. One of the major limitations to current photosensitizers is the drawback of prolonged skin photosensitivity. Compared to Photofrin, the bacteriopurpurinimide **3** produced limited photosensitivity and thus it provides a distinctive advantage over most of the porphyrin-based compounds. Finally, it can easily be derived from the naturally occurring bacteriochlorophyll-a and displays promise as a new PDT agent for the treatment of large and/or deeply seated tumors.

Experimental Section

Chemistry. All chemicals were of reagent grade and used as such. Solvents were dried using standard methods. Reactions were carried out under nitrogen atmosphere and were monitored by precoated (0.20 mm) silica TLC plastic sheet (20 × 20 cm) strips (POLYGRAM SIL N-HR) and/or UV−visible spectroscopy. Silica

gel 60 (70−230 mesh, Merck) was used for column chromatography. UV−visible spectra were recorded on a Varian (Cary-50 Bio) spectrophotometer. ^{1}H NMR spectra were recorded on a Brucker AMX 400 MHz NMR spectrometer at 303 K in $CDCl_3$. Proton chemical shifts (δ) are reported in parts per million (ppm) relative to $CDCl_3$ (7.26 ppm) or TMS (0.00 ppm). Coupling constants (*J*) are reported in Hertz (Hz), and s, d, t, q, p, m, and br refer to singlet, doublet, triplet, quartet, pentet, multiplet, and broad, respectively. Mass spectral analysis was performed in the Biopolymer Facility, Roswell Park Cancer Institute, Buffalo, and Michigan State University, East Lansing, Michigan.

Synthesis of Bacteriopurpurin-18 Methyl Ester (1). *Rb. sphaeroides* (∼1.5 kg) and ∼3000 mL of 1-propanol were stirred overnight with a continuous flow of N_2 gas bubbled through the mixture. The bacterial sludge was filtered through a Buchner funnel, and the blackish-blue/green filtrate was collected (peak absorbance at 776 nm in 1-propanol). A KOH solution was added to the filtrate. With air bubbling through the solution, the reaction was stirred for ∼1 h at rt. The reaction was complete when a wavelength absorption shift occurred from 776 to 768 nm. At this point the mixture was red; however, during transfer to the ice + water solution the mixture turned bluish-green. During stirring, 5% H_2SO_4 was added dropwise until the mixture reached a pH in the range of 2−3 (changed back to dark red hue). The mixture was washed with water and CH_2Cl_2, and the organic layer was collected, dried over Na_2SO_4, and filtered. The filtrate was rotovapped to dryness and refluxed in THF for ∼30 min until a peak at ∼815 nm was noticeable. The mixture was filtered with hexane, and the solid was collected via Buchner funnel filtration. The filtrate mainly containing the carotene analogues was discarded, and the solid isolated as a carboxylic acid analogue was treated with diazomethane and converted into the methyl ester. The crude material was purified on a silica column using 2% acetone in CH_2Cl_2 (yield ∼2.2 g). UV−vis (in CH_2Cl_2): 364 nm ($\epsilon = 8.91 \times 10^4$), 412 nm ($\epsilon = 5.36 \times 10^4$), 545 nm ($\epsilon = 3.4 \times 10^4$), 815 nm ($\epsilon = 5.53 \times 10^4$). ^{1}H NMR (400 MHz, 3 mg/1 mL $CDCl_3$, δ ppm): 9.21 (s, 1H, 5-H), 8.78 (s, 1H, 10-H), 8.62 (s, 1H, 20-H), 5.13 (m, 1H, 17-H), 4.30 (m, 2H, 1H for 7-H, 1H for 18-H), 4.08 (m, 1H, 8-H), 3.63 (s, 3H, 12-CH_3), 3.57 (s, 3H, −$COOCH_3$), 3.52 (s, 3H, 2-CH_3), 3.15 (s, 3H, CH_3C), 2.70 (m, 1H, −C*H*HCH$_2$COOCH_3), 2.42 (m, 2H, 8-C*H*$_2$CH$_3$), 2.35 (m, 1H, −CH*H*CH$_2$COOCH_3), 2.00 (m, 2H, −CH$_2$C*H*$_2$COOCH_3), 1.80 (d, *J* = 7.17 Hz, 3H, 7-CH_3), 1.70 (d, *J* = 6.82 Hz, 3H, 18-CH_3), 1.1 (t, *J* = 6.46 Hz, 3H, 8-CH$_2$C*H*$_3$), −0.03 (s, 1H, NH), −0.65 (s, 1H, NH). Calcd for $C_{34}H_{36}N_4O_6 \cdot H_2O$: C, 66.42; H, 6.24; N, 9.12. Found: C, 66.30; H, 5.90; N, 8.99. Mass calcd for $C_{34}H_{36}N_4O_6$: 596.3. Found: *m*/*e* 596.8 (M + 1). HRMS calcd: 596.2635. Found: 596.2615.

Bacteriopurpurin-18-*N*-3,5-bis(trifluoromethyl) Benzyl Imide Methyl Ester (4). Compound **1** (250 mg, 0.42 mmol) and 3,5-bis-(trifluoromethyl)benzylamine (3 g, 0.012 mol) were refluxed in 25 mL of dry benzene under N_2 gas for ∼24 h. The reaction was washed with water and CH_2Cl_2. The organic layer was collected, dried over Na_2SO_4, and concentrated under vacuum. The residue was found to be a mixture of mainly two compounds, exhibiting 2 absorption bands at 799 and 826 nm. The compounds were separated by preparative TLC and were identified as compounds **2** and **4**, respectively. The yield of the individual product was found to depend on the reaction conditions. Dissolving the mixture in CH_2Cl_2 and subsequent treatment with dilute HCl converted the majority of product to bacteriopurpurinimide **4**, which yielded a single peak at 826 nm. The reaction product was immediately washed with water and CH_2Cl_2 (3 × 100 mL), and the organic layer was collected, dried over Na_2SO_4, and concentrated under vacuum. The crude material was purified on silica prep plates using 1% acetone in CH_2Cl_2 (yield: 245 mg, 71%). UV−vis (ϵ = 59,500 at 820 in THF): 544.9 (3.19×10^4), 414.9 (3.87×10^4), 363.9 (7.45×10^4). ^{1}H NMR (400 MHz, 3 mg/1 mL $CDCl_3$, δ ppm): 9.20 (s, 1H, 5-H); 8.80 (s, 1H, 10-H); 8.60 (s, 1H, 20-H); 8.19 (s, 2H, Ar−H); 7.80 (s, 1H, Ar−H); 5.74 (s, 2H, NC*H*$_2$Ar); 5.25 (m, 1H, 17-H); 4.22−4.32 (m, 2H, 7-H and 18-H); 4.05−4.15 (m, 1H, 8-H); 3.70 (s, 3H, 12-CH_3); 3.55 (s, 3H, 17^{2}CO$_2$-CH_3); 3.54 (s, 3H, 2-CH_3); 3.17 (s, 3H, 3-$COCH_3$); 2.60−2.70 (m, 1H, 1 × 17^{1}H); 2.43 (m, 3H, 8^{1}C*H*$_2$ and 1 × 17^{1}H); 2.00−2.10 (m, 1H, 1 × 17^{2}H); 1.85−1.95 (m, 1H, 1 × 17^{2}H); 1.81 (d, *J* = 5.8, 3H, 7-CH_3); 1.72 (d, *J* = 6.9, 3H, 18-CH_3); 1.10 (t, *J* = 7.0, 3H, 8^{2}C*H*$_3$); −0.35 (brs, 1H, NH); −0.61 (brs, 1H, NH). Mass calculated for $C_{43}H_{41}N_5O_5F_6$: 821.30. Found: 844.4 (M + Na). HRMS calcd: 821.3012. Found: 822.3090.

3-Deacetyl-3-[1^1-3,5-bis(trifluoromethyl)benzylenium]ethyl-purpurin-18-*N*-3,5-bis(trifluoromethyl)benzyl Imide (2). Reaction of **1** (250 mg, 0.42 mmol) with a melt of 3,5-bis(trifluoromethyl)-benzylamine (3 g, 0.012 mol) under N_2 gas at refluxing conditions for 60−70 min afforded mainly compound **2.** The crude material was purified on silica prep plates in 1% acetone in CH_2Cl_2 (yield 50%). UV−vis (ϵ = 50 900 at 803 in CH_2Cl_2): 739 (1.34×10^4), 538.9 (3.6×10^4), 473 (5.80×10^3), 418.9 (5.09×10^4), 369.0 (1.00×10^5). ^{1}H NMR (400 MHz, 3 mg/1 mL $CDCl_3$, δ ppm): 8.76 (s, 1H, 10-H), 8.66 and 8.70 (each singlet for 0.5 H, 5-H), 8.50 (s, 1H, 20-H), 8.22 (s, 4H, ArH), 8.22 (s, 1H, ArH), 8.12 (two close singlets, 1H, ArH), 8.12 (two close singlets, 1H, ArH), 7.82 (2H, −C═N−CH$_2$−), 5.76 (2H, −C−NH−C*H*$_2$−), 5.20 (m, 1H, 17-H), 4.25 (m, 3H, 3H, 1H for 7-H, 1H for 8-H, 1H for 18-H), 3.68 (s, 3H, 12-H), 3.56 (s, 6H, 3H for −$COOCH_3$, 3H for 3^1-CH_3), 3.18 (s, 3H, 2-CH_3), 2.70 (m, 1H, −C*H*HCH$_2$COOC$_3$H$_7$), 2.30 (m, 3H, 1H for −CH*H*CH$_2$COOC$_3$H$_7$, 2H for 8-C*H*$_2$CH$_3$), 1.80 (d, *J* = 6.90 Hz, 3H, 7-CH_3), 1.70 (d, *J* = 6.91 Hz, 3H, 18-CH_3), 1.61 (m, 2H, −CH$_2$C*H*$_2$COOC$_3$H$_7$), 1.20 (t, *J* = 6.89 Hz, 3H, 8-CH$_2$C*H*$_3$), −0.1, −0.3, −0.4, −0.6 (each singlet for 0.5 H, NH). Mass calculated for $C_{52}H_{46}N_6O_4F_{12}$: 1046.34. Found: 1069.5 (M + Na). HRMS calcd: 1046.3389. Found: 1047.3470.

3-Deacetyl-3-[1′-3,5-bis(trifluoromethyl) benzylamine]-purpurin-18-*N*-3,5-bis(trifluoromethyl) Benzyl Imide (3). The Schiff base **2** (28 mg, 0.027 mmol) was dissolved in 15 mL of dry CH_2Cl_2 and reacted with 45 mg of $NaBH_4$, and 5 mL of MeOH was added. After stirring for 15−30 min, additional $NaBH_4$ was added until the reaction was complete (determined by UV−vis spectroscopy and analytical TLC). The reaction mixture was diluted with water, and a small amount of 2% acetic acid was added (pH = 5). The reaction mixture was washed with water and CH_2Cl_2 (3 × 100 mL), and the organic layer was collected, dried over Na_2SO_4, and concentrated under vacuum. The crude material was purified on silica prep plates using 1.5% MeOH in CH_2Cl_2 (yield 75%). UV−vis 790 nm (ϵ = 38 600 in THF): 538.0 (3.99×10^4), 506 (6.09×10^3), 470.0 (5.22×10^3), 417.0 (5.2×10^4), 367.0 (9.97×10^4). ^{1}H NMR (400 MHz, 3 mg/1 mL $CDCl_3$, δ ppm): 9.12, 9.05 (each singlet for 0.5 H, 5-H), 8.60 (s, H-10), 8.30 (two close singlets, 1H, ArH), 8.20 (s, 2H, ArH), 7.80 (s, 2H, ArH), 7.70 (two close singlets, H-20), 5.70 (two close singlets, 2H, imide ring N−CH$_2$), 5.2 (m, 2H, 3^1-H and 17-H), 4.20 (m, 2H, 3^1-N−CH$_2$−), 4.05 (m, 3H, 3H, 1H for 7-H, 1H for 8-H, 1H for 18-H), 3.60 (s, 3H, 12-H), 3.58 (s, 3H, −$COOCH_3$), 3.20 (s, 3H, 20-CH_3), 2.60 (m, 1H, −C*H*HCH$_2$COOC$_3$H$_7$), 2.30 (m, 3H, 1H for −CH*H*CH$_2$COOC$_3$H$_7$, 2H for 8-C*H*$_2$CH$_3$), 2.00 (d, *J* = 6.8 Hz, 3^1-CH_3), 1.80 (d, *J* = 6.90 Hz, 3H, 7-CH_3), 1.70 (d, *J* = 6.91 Hz, 3H, 18-CH_3), 1.61 (m, 2H, −CH$_2$C*H*$_2$COOC$_3$H$_7$), 1.20 (t, *J* = 6.89 Hz, 3H, 8-CH$_2$C*H*$_3$), 0.30, −0.05 (each singlet for 1H, NH). Mass calculated for $C_{52}H_{48}N_6O_4F_{12}$: 1048.35. Found: 1049.3 (M + 1). HRMS calcd: 1048.3545. Found: 1049.3620.

Formulation of Bacteriopurpurinimides. The bacteriopurpurinimides derived from bacteriopurpurin-18 methyl ester were insoluble in water; therefore for biological studies these compounds were dissolved in 1% Tween 80 (Sigma) and 5% dextrose solution (Baxter Healthcare corporation). The concentration of the photosensitizers in the solutions was determined by using the Beer−Lambert law equation.[29]

HPLC Analysis of Bacteriopurpurinimides. Analytical separations were performed on a 5 μm LiChroCART 100 RP-8 25 cm column. The photosensitizers **2**, **3**, and **4** were formulated in 1% Tween 80/D5W and analyzed over a mobile phase gradient from 90% MeOH to 100% MeOH at a flow rate of 1.50 mL/min (time 0−10 min, 10% H_2O, 90% MeOH; 10−20 min, 5% H_2O, 95% MeOH; 20−30 min, 100% MeOH.

Animals and Tumor System. Female C3H mice (10−16 weeks old; weight range 18−25 g) obtained from NCI were used for in vivo studies. Approximately 3×10^5 radiation induced fibrosarcoma (RIF; murine tumor cell line) tumor cells were implanted subcutaneously on the axilla of the mouse. After 5−7 days the tumors reached 4−6 mm in size and were suitable for experiments. All experiments were carried out and maintained according to RPCI IACUC and DLAR regulations.

In Vitro PDT. The RIF tumor cells grown in alpha-minimum essential medium (α-MEM) with 10% fetal calf serum, L-glutamine, and penicillin/streptomycin/neomycin were maintained in 5% CO_2, 95% air, and 100% humidity. These cells were plated in 96-well plates at a density of 5×10^3 cells/well in complete media as a means to determine PDT efficacy. The next day, photosensitizer **3** was added at variable concentrations (1.25−20 μM). After the 24 h incubation in the dark at 37 °C, the cells were replaced with complete media and exposed to light at a dose rate of 3.2 mW/cm^2 at various light doses (1−20 J). The dye laser (375; Spectra Physics, Mt. View, CA) excited by an argon-ion laser (171 laser; Spectra-Physics, Mt. View, CA) was tuned to emit the drug-activating wavelength 796 nm. Uniform illumination was accomplished using a 600 μm diameter quartz optical fiber fitted with a graded index refraction lens. Following illumination, the plates were incubated at 37 °C in the dark for 48 h. Appropriate dark controls at variable drug doses were also included. Following the 48 h incubation in the dark the plates were evaluated for cell viability using the MTT assay. PDT phototoxicity for compound **4** was not evaluated at this time due to laser limitations (could not tune laser to ∼824 nm with enough power to perform experiments).

Cell Viability Assay. Cell viability was measured using the 3-[4,5-dimethylthiazol-2-yl]-2,5-diphenyl tetrazoliumbromide (MTT) assay.[20] Immediately following light treatment, the cells were incubated for 48 h in the dark at 37 °C. After 48 h, 10 μL of 4.0 mg/mL solution of MTT dissolved in PBS (Sigma Chemical Co., St. Louis, MO) was added to each well. After the 4 h MTT incubation, the MTT + media were removed and 100 μL of dimethyl sulfoxide was added to solubilize the formazin crystals. The PDT efficacy was measured by reading the 96-well plate on a microtiter plate reader (Miles Inc., Titertek Multiscan Plus MK II) at an absorbance of 560 nm. The results were plotted as percent survival compared with the corresponding dark control (drug, no light) for each compound tested. Each data point represents the mean from a typical experiment with four replicate wells, and the error bars are the standard deviation from three separate experiments.

Intracellular Localization Using Fluorescence Microscopy. RIF cells were seeded on poly-L-lysine coated glass coverslips at 1×10^5 in 6-well plates and cultured in α-MEM for 48 h to allow for attachment and spreading.[21] Photosensitizer **3** at 1.0 μM was incubated in the dark at 37 °C for 24 h. Cells + photosensitizer were additionally incubated with the mitochondria localizing dye, MitoTracker Green (λ_{ex} = 490 nm, λ_{em} = 516 nm) (Molecular Probes, Eugene, OR) for 24 h. Prior to microscopy the cells were gently rinsed with PBS. A fluorescence microscope with filter cube containing 530−585 nm excitation filter, and a 600 nm dichroic filter and a 615 nm long-pass emission filter were utilized for detection of the photosensitizer. MitoTracker Green was detected using a 450−490 nm excitation filter, and a 510 nm dichroic filter with a 520−560 nm long-pass emission filter. Fluorescent images were captured and analyzed with a CCD camera and intensifier as previously described.[22] Images of photosensitizers and MitoTracker Green localization were taken in rapid succession.

Drug Uptake by in Vivo Reflectance Spectroscopy. For determining the in vivo drug uptake, the C3H mice with RIF tumors (5−6 mm^3) were first anesthetized using ketamine xylazine intraperitoneally. The optical power as a function of wavelength was recorded before the iv injection of the photosensitizer.[23] The measurements were acquired through the use of bundle optical fibers that were positioned on the surface of the tumor (RIF) plus overlying skin and normal skin (C3H). The drug at 5.0 μmol/kg was then injected (via orbital plexus) and the absorbance spectrum of the drug postinjection was recorded over time (up to 2 days postinjection). The in vivo drug absorption spectrum was best displayed by determining the ratio of the postinjection spectrum to the preinjection spectrum in the tumor versus the skin. This experiment determined the wavelength and time at which to perform the in vivo PDT treatment.

Evaluation of in Vivo Photosensitizing Efficacy. The stable bacteriopurpurinimide **3** was evaluated for in vivo tumor response in C3H mice bearing RIF tumors. In brief, C3H mice (5 mice/group) were injected subcutaneously in the axilla with 3×10^5 RIF cells in 40 μL of complete α-MEM and permitted to grow until they were 4−5 mm in diameter. The day before PDT light treatment, the mice were injected intravenously with either 0.2, 0.4, or 1.0 μmol/kg of the photosensitizer. At 24 h postinjection, the mice were restrained in plastic holders without anesthesia and treated with a 1 cm^2 drug-activating laser light area (796 nm) from an argon-pumped dye laser for a total fluence of 135 J/cm^2 at a fluence rate of 75 mW/cm^2. Post-PDT, the mice were observed daily, the tumors were measured using two orthogonal measurements L and W (perpendicular to L), and the volumes were calculated using the formula $V = LW^2/2$ and recorded. Mice were considered cured if there was no palpable tumor by day 90. At this time bacteriopurpurinimide **2** was not evaluated due to limitations in our laser diode resources (not feasible to treat more than 1 mouse at a time).

Fluorescein-Exclusion Assay for Vascular Stasis. The day before PDT light treatment, bacteriopurpurinimde **3** at 1.0 μmol/kg was injected intravenously. At 24 h postinjection, the mice (not inoculated with RIF) underwent PDT as described above. The mice were evaluated for PDT-induced vascular shutdown at various time points post-PDT (1, 4, and 24 h).[24] At each time point, 3 mice/group were injected iv with 0.20 cm^3 of fluorescein (λ_{ex} = 490 nm, λ_{em} = 520 nm), which has a very short plasma distribution half-life, and the vascular damage was evaluated 2−5 min postinjection. An in vivo fluorescence probe was utilized to quantitate fluorescein fluorescence in the treatment site (1 cm^2 area) as compared to the hind-leg non light treatment site.

Histological Analysis of Tumor Response. The day before PDT light treatment, bacteriopurpurinimde **3** at 1.0 μmol/kg was injected intravenously into C3H mice bearing RIF tumors. At 24 h postinjection, the mice underwent PDT as described above (796 nm; 135 J/cm^2 at 75 mW/cm^2). At various time points post-PDT, the mice were euthanized and their tumors were removed, fixed in zinc, dehydrated with 70% EtOH, and embedded in paraffin. For histological examination of tumor response post-PDT, the sections were stained with hematoxylin and eosin (H&E) and CD31 (stains endothelial blood vessels). Tumor samples were evaluated under a Zeiss light microscope (20- or 40-fold magnification), and photographs were taken using the AxioVision LE Application V9.1.

Skin Photosensitivity. One of the major problems associated with porphyrin-based compounds is long-lasting skin photosensitivity. The foot-pad of SWISS/Cr mice was utilized for determining drug + light photosensitivity.[26] Bacteriopurpurinimde **3** was evaluated at a dose of 1.0 μmol/kg (therapeutic dose). For example, all six SWISS/Cr mice were injected with **3** on the same day. At 24, 48, 72, and 96 h postinjection the mouse was restrained on a board without anesthesia and its foot (3 feet/time point) was exposed to solar simulated light for 30 min. Following illumination, the foot was monitored daily on a scale of 0−3 for skin sensitivity. Foot response was judged using a 0−3 scale (0.1 = no apparent difference from normal, 0.3 = slight edema, 0.5 = moderate edema, 0.75 = large edema, 1.0 = large erythema with exudates, 1.2 = moderate edema with slight scaly or crusty appearance, 1.5 = definite erythema and definite scaly or crusty appearance, 1.65 = slight damage and or slight fusion of toes, 2.0 = most toes fused but no change in general shape, 2.5 = foot shapeless with no toes, 3.0 = only sub of foot remaining; a response score >2.0 indicates unacceptably severe normal tissue reaction).

Instrumentation and Methods for Photophysical Studies. Steady-state measurements at room temperature were performed using a Shimadzu UV-3101PC spectrophotometer (absorption

spectra) and Fluorolog-3 spectrofluorometer (Jobin Yvon) (fluorescence spectra).

A SPEX 270M spectrometer (Jobin Yvon) equipped with an InGaAs photodetector (Electro-Optical Systems Inc.) was used for acquisition of singlet oxygen emission spectra in organic solvents. A diode pumped solid-state laser (Verdi, Coherent) at 532 nm was the excitation source. The sample solution in a quartz cuvette was placed directly in front of the entrance slit of the spectrometer, and the exciting laser beam was directed at 90° relative to the collection of emission. Long-pass filters, 538AELP and 950 LP (Omega Optical), were used to attenuate the excitation laser light and fluorescence from the samples.

Acknowledgment. The financial support from the NIH (CA55791, IR 21 CA109914-01) and the shared resources of the RPCI Support Grant P30CA16056 is highly appreciated. A.L.G. thanks the National Science Foundation under the Integrative Graduate Education and Research Traineeship (Grant DGE0114330) for funding the graduate fellowship.

References

(1) Dougherty, T. J.; Levy, J. G. Photodynamic Therapy (PDT) and Clinical Applications. In *Biomedical Photonics Handbook*; Vo-Dinh, T., Ed.; CRC Press: Boca Raton, 2002.

(2) Schmidt-Erfurth, U.; Diddens, H.; Birngruber, R.; Hasan, T. Photodynamic Targeting of Human Retinoblastoma Cells Using Covalent Low-Density Lipoprotein Conjugates. *Br. J. Cancer* **1997**, *75*, 54−61.

(3) (a) Oleinick, N. L.; Morris, R. L.; Belichenko, T. The Role Apoptosis in Response of Photodynamic Therapy: What, Where, Why and How? *Photochem. Photobiol. Sci*. **2002**, *1*, 1−21. (b) Osterloh, J.; Vicente, M. G. H. Mechanisms of Porphyrinoid Localization in Tumors. *J. Porphyrins Phthalocyanines* **2002**, *6* (5), 305−324.

(4) Dolmans, D. E.; Fukumura, D.; Jain, R. K. Photodynamic Therapy of Cancer. *Nat. Rev. Cancer* **2003**, *3* (5), 380.

(5) Weishaupt, K. R.; Gomer, C. J.; Dougherty, T. J. Identification of Singlet Oxygen as the Cytotoxic Agent in Photo-Inactivation of a Murine Tumor. *Cancer Res*. **1976**, *36*, 2326−2329.

(6) Sharman, W. M.; Allen, C. M.; van Lier, J. E. Role of Activated Oxygen Species in Photodynamic Therapy. *Methods Enzymol*. **2000**, *319*, 376−400.

(7) Wilson, B. C.; Patterson, M. S.; Lilge, L. Implicit and Explicit Dosimetry in Photodynamic Therapy: A New Paradigm. *Lasers Med. Sci*. **1997**, *12*, 182−199.

(8) Lobel, J.; MacDonald, I. J.; Ciesielski, M. J.; Barone, T.; Potter, W. R.; Pollina, J.; Plunkett, R. J.; Fenstermaker, R. A.; Dougherty, T. J. 2-[1-Hexyloxyethyl]-2-devinylpyropheophorbide-a (HPPH) in a Nude Rat Glioma Model: Implications for Photodynamic Therapy. *Lasers Surg. Med.* **2001**, *29*, 397−405.

(9) Pandey, R. K.; Zheng, G. *Applications: Past, Present and Future*, Vol. 6 of *The Porphyrin Handbook*; Kadish, K., Smith, K., Guilard, R., Eds.; Academic Press: San Diego, 2002.

(10) Ali, H.; van Lier, J. E. Metal Complexes as Photo and Radiosensitizers. *Chem. Rev*. **1999**, *99*, 2329−2450.

(11) Henderson, B. W.; Bellnier, D. A.; Graco, W. R.; Sharma, A.; Pandey, R. K.; Weishaupt, K. R.; Dougherty, T. J. A Quantitative Structure−Activity Relationship for a Cogeneric Series of Pyropheophorbide-a Derivatives as Photosensitizers for Photodynamic Therapy. *Cancer Res*. **1997**, *57*, 4000−4007.

(12) Zheng, G.; Camacho, S.; Potter, W.; Bellnier, D. A.; Henderson, B. W.; Dougherty, T. J.; Pandey, R. K. Synthesis, Tumor Uptake and in Vivo Photosensitizing Efficacy of a Homologous Series of the 3-(1′-Alkoxy)ethyl-purpurin-18-*N*-alkylimides. *J. Med. Chem.* **2001**, *44*, 1540−1559.

(13) He, J.; Larkin, H. E.; Li, Y. S.; Rihter, B. D.; Zaidi, S. I. A.; Rodgers, M. A. J.; Mukhtar, H.; Kenney, M. E.; Oleinick, N. L. The Synthesis, Photophysical and Photobiological Properties and in Vitro Structure−Activity Relationships of a Set of Silicon Phthalocyanine PDT Photosensitizers. *Photochem. Photobiol*. **1997**, *65*, 581−586.

(14) Bonnett, R.; Ioannou, S.; White, R. D.; Winfield, U. J.; Berenbaum, M. C. Meso Tetra(hydroxyphenyl) Porphyrins as Tumor Photosensitizers, Chemical and Photochemical Aspects. *Photochem. Photobiol.* **1987**, 45−56.

(15) Chen, Y.; Li, G.; Pandey, R. K. Synthesis of Bacteriochlorins and Their Potential Utility in Photodynamic Therapy (PDT). *Curr. Org. Chem.* **2004**, *8* (12), 1105−1134.

(16) Chen, Y.; Graham, A.; Potter, W.; Morgan, J.; Vaughan, L.; Bellnier, D. A.; Henderson, B. W.; Oseroff, A.; Dougherty, T. J.; Pandey, R. K. Highly Stable and Potent Photosensitizers for Photodynamic Therapy. *J. Med. Chem.* **2003**, *45* (2), 255−258.

(17) Gryshuk, A. L.; Graham, A.; Pandey, S. K.; Potter, W. R.; Oseroff, A.; Dougherty, T. J.; Pandey, R. K. A First Comparative Study of Purpurinimide-Based Fluorinated vs Nonfluorinated Photosensitizers for Photodynamic Therapy. *Photochem. Photobiol.* **2002**, *76* (5), 555−559.

(18) Kozyrev, A. N.; Zheng, G.; Zhu, C. F.; Dougherty, T. J.; Smith, K. M.; Pandey, R. K. Synthesis of Stable Bacteriochlorophyll-a Derivatives as Potential Photosensitizers for PDT. *Tetrahedron Lett.* **1996**, *37*, 6431−6434.

(19) Wilson, B. C.; Farrell, T. J.; Patterson, M. S. An Optical Fiber-Based Diffuse Reflectance Spectrometer for Non-Invasive Investigations of Photodynamic Sensitizers *in Vivo*. In *Future Directions and Applications in Photodynamic Therapy*; *Proc. SPIE, Bellingham, Washington*, Vol. IS6; Gomer, C. J., Ed.; 1990, pp 219−232.

(20) Morgan, J.; Potter W. R.; Oseroff A. R. Comparison of Photodynamic Targets in a Carcinoma Cell Line and Its Mitochondrial DNA-Deficient Derivative. *Photochem. Photobiol.* **2000**, *70*, 747−757.

(21) Kessel, D.; Luo, Y.; Deng, Y.; Chang C. K. The Role of Subcellular Localization in Inhibition of Apotosis by Photodynamic Therapy. *Photochem. Photobiol.* **1997**, *65* (3), 422−426.

(22) Almeida, R. D.; Manadas, B. J.; Carvalho, A. P.; Duarte, C. B. Intracellular Signaling Mechanisms in Photodynamic Therapy. *Biochim. Biophys. Acta* **2004**, 59−86.

(23) Fingar, V. H.; Kik, P. K.; Haydon, P. S.; Cerrito, P. B.; Tseng, M.; Aband, E.; Wieman, T. J. Analysis of Acute Vascular Damage after Photodynamic Therapy Using Benzoporphyrin Derivative (BPD). *Br. J. Cancer* **1999**, *79*, 1702−1708.

(24) Bellnier, D. A.; Potter, W. R.; Vaughan, L. A.; Sitnik, T. M.; Parsons, J. C.; Greco, W. R.; Whitaker, J.; Johnson, P.; Henderson, B. W. The Validation of a New Vascular Damage Assay for PDT Agents. *Photochem. Photobiol*. **1995**, *62* (5), 896−905.

(25) Fabris, C.; Valduga, G.; Miotto, G.; Borsetto, L.; Jori, G.; Garbisa, S.; Reddi, E. Photosensitization with Zinc(II)Phthalocyanine as a Switch in the Decision between Apoptosis and Necrosis. *Cancer Res.* **2001**, *61*, 7495−7500.

(26) Henderson, B. W.; Bellnier, D. A. Tissue Localization of Photosensitizers and the Mechanism of Photodynamic Tissue Destruction. *Ciba Found. Symp.* **1989**, *146*, 112−25.

(27) Magde, D.; Wong, R.; Sybold, P. G. Fluorescence Quantum Yields and Their Relation to Lifetimes of Rhodamine 6G and Fluorescein in Nine Solvents: Improved Absolute Standards for Quantum Yields. *Photochem. Photobiol*. **2002**, *75* (4), 327−334.

(28) Demas, J. N.; Harris, E. W.; McBride, R. P. *Energy Transfer from Luminescent Transition Metal Complexes to Oxygen. J. Am. Chem. Soc*. **1977**, *99*, 3547−3551.

(29) Kalsi, P. S. *Spectroscopy of Organic Compounds*; Wiley Eastern: New Delhi, 1993.

JM050919Z